EUROPEAN LABORATORY FOR PARTICLE PHYSICS (CERN)

CERN-EP/98-053
8th April 1998

Single- and multi-photon production in e^+e^- collisions at a centre-of-mass energy of 183 GeV

The ALEPH Collaboration

Abstract

The production of final states involving one or more energetic photons from e^+e^- collisions is studied in a sample of $58.5\,pb^{-1}$ of data recorded at a centre-of-mass energy of 183 GeV by the ALEPH detector at LEP. The $e^+e^- \to \nu\bar{\nu}\gamma(\gamma)$ and $e^+e^- \to \gamma\gamma(\gamma)$ cross sections are measured. The data are in good agreement with predictions based on the Standard Model and are used to set upper limits on the cross sections for anomalous photon production in the context of two supersymmetric models and for various extensions to QED. In particular, in the context of a super-light gravitino model a cross section upper limit of 0.38 pb is placed on the process $e^+e^- \to \tilde{G}\tilde{G}\gamma$, allowing a lower limit to be set on the mass of the gravitino. Limits are also set on the mass of the lightest neutralino in Gauge Mediated Supersymmetry Breaking models. In the case of equal $ee^*\gamma$ and $ee\gamma$ couplings a 95% C.L. lower limit on M_{e^*} of $250\,GeV/c^2$ is obtained.

(To be submitted to Physics Letters B)

The ALEPH Collaboration

R. Barate, D. Buskulic, D. Decamp, P. Ghez, C. Goy, S. Jezequel, J.-P. Lees, A. Lucotte, F. Martin, E. Merle, M.-N. Minard, J.-Y. Nief, B. Pietrzyk

Laboratoire de Physique des Particules (LAPP), IN^{2}P^3-CNRS, F-74019 Annecy-le-Vieux Cedex, France

R. Alemany, G. Boix, M.P. Casado, M. Chmeissani, J.M. Crespo, M. Delfino, E. Fernandez, M. Fernandez-Bosman, Ll. Garrido,[15] E. Graugès, A. Juste, M. Martinez, G. Merino, R. Miquel, Ll.M. Mir, P. Morawitz, I.C. Park, A. Pascual, J.A. Perlas, I. Riu, F. Sanchez

Institut de Física d'Altes Energies, Universitat Autònoma de Barcelona, 08193 Bellaterra (Barcelona), E-Spain[7]

A. Colaleo, D. Creanza, M. de Palma, G. Gelao, G. Iaselli, G. Maggi, M. Maggi, S. Nuzzo, A. Ranieri, G. Raso, F. Ruggieri, G. Selvaggi, L. Silvestris, P. Tempesta, A. Tricomi,[3] G. Zito

Dipartimento di Fisica, INFN Sezione di Bari, I-70126 Bari, Italy

X. Huang, J. Lin, Q. Ouyang, T. Wang, Y. Xie, R. Xu, S. Xue, J. Zhang, L. Zhang, W. Zhao

Institute of High-Energy Physics, Academia Sinica, Beijing, The People's Republic of China[8]

D. Abbaneo, U. Becker, P. Bright-Thomas, D. Casper, M. Cattaneo, V. Ciulli, G. Dissertori, H. Drevermann, R.W. Forty, M. Frank, F. Gianotti, R. Hagelberg, J.B. Hansen, J. Harvey, P. Janot, B. Jost, I. Lehraus, P. Maley, P. Mato, A. Minten, L. Moneta,[20] N. Qi, A. Pacheco, F. Ranjard, L. Rolandi, D. Rousseau, D. Schlatter, M. Schmitt,[1] O. Schneider, W. Tejessy, F. Teubert, I.R. Tomalin, M. Vreeswijk, H. Wachsmuth

European Laboratory for Particle Physics (CERN), CH-1211 Geneva 23, Switzerland

Z. Ajaltouni, F. Badaud G. Chazelle, O. Deschamps, A. Falvard, C. Ferdi, P. Gay, C. Guicheney, P. Henrard, J. Jousset, B. Michel, S. Monteil, J-C. Montret, D. Pallin, P. Perret, F. Podlyski, J. Proriol, P. Rosnet

Laboratoire de Physique Corpusculaire, Université Blaise Pascal, IN^{2}P^3-CNRS, Clermont-Ferrand, F-63177 Aubière, France

J.D. Hansen, J.R. Hansen, P.H. Hansen, B.S. Nilsson, B. Rensch, A. Wäänänen

Niels Bohr Institute, 2100 Copenhagen, DK-Denmark[9]

G. Daskalakis, A. Kyriakis, C. Markou, E. Simopoulou, A. Vayaki

Nuclear Research Center Demokritos (NRCD), GR-15310 Attiki, Greece

A. Blondel, J.-C. Brient, F. Machefert, A. Rougé, M. Rumpf, R. Tanaka, A. Valassi,[6] H. Videau

Laboratoire de Physique Nucléaire et des Hautes Energies, Ecole Polytechnique, IN^{2}P^3-CNRS, F-91128 Palaiseau Cedex, France

E. Focardi, G. Parrini, K. Zachariadou

Dipartimento di Fisica, Università di Firenze, INFN Sezione di Firenze, I-50125 Firenze, Italy

R. Cavanaugh, M. Corden, C. Georgiopoulos, T. Huehn, D.E. Jaffe

Supercomputer Computations Research Institute, Florida State University, Tallahassee, FL 32306-4052, USA [13,14]

A. Antonelli, G. Bencivenni, G. Bologna,[4] F. Bossi, P. Campana, G. Capon, F. Cerutti, V. Chiarella, G. Felici, P. Laurelli, G. Mannocchi,[5] F. Murtas, G.P. Murtas, L. Passalacqua, M. Pepe-Altarelli

Laboratori Nazionali dell'INFN (LNF-INFN), I-00044 Frascati, Italy

M. Chalmers, L. Curtis, A.W. Halley, J.G. Lynch, P. Negus, V. O'Shea, C. Raine, J.M. Scarr, K. Smith, P. Teixeira-Dias, A.S. Thompson, E. Thomson, J.J. Ward

Department of Physics and Astronomy, University of Glasgow, Glasgow G12 8QQ,United Kingdom[10]

O. Buchmüller, S. Dhamotharan, C. Geweniger, G. Graefe, P. Hanke, G. Hansper, V. Hepp, E.E. Kluge, A. Putzer, J. Sommer, K. Tittel, S. Werner, M. Wunsch

Institut für Hochenergiephysik, Universität Heidelberg, D-69120 Heidelberg, Germany[16]

R. Beuselinck, D.M. Binnie, W. Cameron, P.J. Dornan,[12] M. Girone, S. Goodsir, E.B. Martin, N. Marinelli, A. Moutoussi, J. Nash, J.K. Sedgbeer, P. Spagnolo, M.D. Williams

Department of Physics, Imperial College, London SW7 2BZ, United Kingdom[10]

V.M. Ghete, P. Girtler, E. Kneringer, D. Kuhn, G. Rudolph

Institut für Experimentalphysik, Universität Innsbruck, A-6020 Innsbruck, Austria[18]

A.P. Betteridge, C.K. Bowdery, P.G. Buck, P. Colrain, G. Crawford, A.J. Finch, F. Foster, G. Hughes, R.W.L. Jones, A.N. Robertson, M.I. Williams

Department of Physics, University of Lancaster, Lancaster LA1 4YB, United Kingdom[10]

I. Giehl, C. Hoffmann, K. Jakobs, K. Kleinknecht, G. Quast, B. Renk, E. Rohne, H.-G. Sander, P. van Gemmeren, C. Zeitnitz

Institut für Physik, Universität Mainz, D-55099 Mainz, Germany[16]

J.J. Aubert, C. Benchouk, A. Bonissent, G. Bujosa, J. Carr,[12] P. Coyle, A. Ealet, D. Fouchez, O. Leroy, F. Motsch, P. Payre, M. Talby, A. Sadouki, M. Thulasidas, A. Tilquin, K. Trabelsi

Centre de Physique des Particules, Faculté des Sciences de Luminy, IN^{2}P^3-CNRS, F-13288 Marseille, France

M. Aleppo, M. Antonelli, F. Ragusa

Dipartimento di Fisica, Università di Milano e INFN Sezione di Milano, I-20133 Milano, Italy.

R. Berlich, W. Blum, V. Büscher, H. Dietl, G. Ganis, H. Kroha, G. Lütjens, C. Mannert, W. Männer, H.-G. Moser, S. Schael, R. Settles, H. Seywerd, H. Stenzel, W. Wiedenmann, G. Wolf

Max-Planck-Institut für Physik, Werner-Heisenberg-Institut, D-80805 München, Germany[16]

J. Boucrot, O. Callot, S. Chen, M. Davier, L. Duflot, J.-F. Grivaz, Ph. Heusse, A. Höcker, A. Jacholkowska, M. Kado, D.W. Kim,[2] F. Le Diberder, J. Lefrançois, L. Serin, E. Tournefier, J.-J. Veillet, I. Videau, D. Zerwas

Laboratoire de l'Accélérateur Linéaire, Université de Paris-Sud, IN^{2}P^3-CNRS, F-91405 Orsay Cedex, France

P. Azzurri, G. Bagliesi,[12] S. Bettarini, T. Boccali, C. Bozzi, G. Calderini, R. Dell'Orso, R. Fantechi, I. Ferrante, A. Giassi, A. Gregorio, F. Ligabue, A. Lusiani, P.S. Marrocchesi, A. Messineo, F. Palla, G. Rizzo, G. Sanguinetti, A. Sciabà, G. Sguazzoni, R. Tenchini, C. Vannini, A. Venturi, P.G. Verdini

Dipartimento di Fisica dell'Università, INFN Sezione di Pisa, e Scuola Normale Superiore, I-56010 Pisa, Italy

G.A. Blair, L.M. Bryant, J.T. Chambers, J. Coles, M.G. Green, T. Medcalf, P. Perrodo, J.A. Strong, J.H. von Wimmersperg-Toeller

Department of Physics, Royal Holloway & Bedford New College, University of London, Surrey TW20 OEX, United Kingdom[10]

D.R. Botterill, R.W. Clifft, T.R. Edgecock, S. Haywood, P.R. Norton, J.C. Thompson, A.E. Wright

Particle Physics Dept., Rutherford Appleton Laboratory, Chilton, Didcot, Oxon OX11 OQX, United Kingdom[10]

B. Bloch-Devaux, P. Colas, B. Fabbro, G. Faïf, E. Lançon,[12] M.-C. Lemaire, E. Locci, P. Perez, H. Przysiezniak, J. Rander, J.-F. Renardy, A. Rosowsky, A. Roussarie, A. Trabelsi, B. Vallage

CEA, DAPNIA/Service de Physique des Particules, CE-Saclay, F-91191 Gif-sur-Yvette Cedex, France[17]

S.N. Black, J.H. Dann, H.Y. Kim, N. Konstantinidis, A.M. Litke, M.A. McNeil, G. Taylor

Institute for Particle Physics, University of California at Santa Cruz, Santa Cruz, CA 95064, USA[19]

C.N. Booth, C.A.J. Brew, S. Cartwright, F. Combley, M.S. Kelly, M. Lehto, J. Reeve, L.F. Thompson

Department of Physics, University of Sheffield, Sheffield S3 7RH, United Kingdom[10]

K. Affholderbach, A. Böhrer, S. Brandt, G. Cowan, J. Foss, C. Grupen, L. Smolik, F. Stephan

Fachbereich Physik, Universität Siegen, D-57068 Siegen, Germany[16]

G. Giannini, B. Gobbo, G. Musolino

Dipartimento di Fisica, Università di Trieste e INFN Sezione di Trieste, I-34127 Trieste, Italy

J. Putz, J. Rothberg, S. Wasserbaech, R.W. Williams

Experimental Elementary Particle Physics, University of Washington, WA 98195 Seattle, U.S.A.

S.R. Armstrong, E. Charles, P. Elmer, D.P.S. Ferguson, Y. Gao, S. González, T.C. Greening, O.J. Hayes, H. Hu, S. Jin, P.A. McNamara III, J.M. Nachtman,[21] J. Nielsen, W. Orejudos, Y.B. Pan, Y. Saadi, I.J. Scott, J. Walsh, Sau Lan Wu, X. Wu, G. Zobernig

Department of Physics, University of Wisconsin, Madison, WI 53706, USA[11]

[1]Now at Harvard University, Cambridge, MA 02138, U.S.A.
[2]Permanent address: Kangnung National University, Kangnung, Korea.
[3]Also at Dipartimento di Fisica, INFN Sezione di Catania, Catania, Italy.
[4]Also Istituto di Fisica Generale, Università di Torino, Torino, Italy.
[5]Also Istituto di Cosmo-Geofisica del C.N.R., Torino, Italy.
[6]Supported by the Commission of the European Communities, contract ERBCHBICT941234.
[7]Supported by CICYT, Spain.
[8]Supported by the National Science Foundation of China.
[9]Supported by the Danish Natural Science Research Council.
[10]Supported by the UK Particle Physics and Astronomy Research Council.
[11]Supported by the US Department of Energy, grant DE-FG0295-ER40896.
[12]Also at CERN, 1211 Geneva 23,Switzerland.
[13]Supported by the US Department of Energy, contract DE-FG05-92ER40742.
[14]Supported by the US Department of Energy, contract DE-FC05-85ER250000.
[15]Permanent address: Universitat de Barcelona, 08208 Barcelona, Spain.
[16]Supported by the Bundesministerium für Bildung, Wissenschaft, Forschung und Technologie, Germany.
[17]Supported by the Direction des Sciences de la Matière, C.E.A.
[18]Supported by Fonds zur Förderung der wissenschaftlichen Forschung, Austria.
[19]Supported by the US Department of Energy, grant DE-FG03-92ER40689.
[20]Now at University of Geneva, 1211 Geneva 4, Switzerland.
[21]Now at University of California at Los Angeles (UCLA), Los Angeles, CA 90024, U.S.A.

1 Introduction

In the framework of the Standard Model, events in which the only observable final state particles are photons may be produced via two distinct reactions: $e^+e^- \to \nu\bar{\nu}\gamma(\gamma)$ and $e^+e^- \to \gamma\gamma(\gamma)$.

The reaction $e^+e^- \to \nu\bar{\nu}\gamma(\gamma)$ can proceed via two processes which are theoretically well understood: radiative returns to the Z resonance ($e^+e^- \to \gamma Z$) with $Z \to \nu\bar{\nu}$, and t-channel W exchange with photon(s) radiated from the beam electrons or the W. This reaction produces final states where one or more photons are accompanied by significant missing energy. These final states have been studied extensively in e^+e^- annihilations at lower centre-of-mass energies [1, 2]. Such final states are also sensitive to new physics via the reactions $e^+e^- \to XX$ and $e^+e^- \to XY$ where Y is purely weakly interacting and X decays radiatively to Y ($X \to Y\gamma$). In the Minimal Supersymmetric Standard Model (MSSM) Y and X could be the lightest and next-to-lightest neutralinos [3, 4, 5], respectively. In Gauge Mediated Supersymmetry Breaking (GMSB) theories [6] Y and X could be the essentially massless gravitino and the lightest neutralino [7, 8], respectively. In the super-light-gravitino scenario [9] the process $e^+e^- \to \tilde{G}\tilde{G}\gamma$ can have an appreciable cross section.

The CDF collaboration has observed an unusual event with two high energy electrons, two high energy photons, and a large amount of missing transverse energy [10]. The Standard Model explanation for this event has a low probability, but it can be accommodated by the SUSY models mentioned above. The D0 collaboration has also searched for this process [11] and has found no significant excess of events. In the neutralino LSP scenario, the CDF event could be explained by the Drell-Yan process $q\bar{q} \to \tilde{e}\tilde{e} \to ee\chi_2^0\chi_2^0 \to ee\chi_1^0\chi_1^0\gamma\gamma$ [5] where the two χ_1^0's escape detection, resulting in missing transverse energy. If this is the explanation for the CDF event, the best possibility for discovery at LEP2 is $e^+e^- \to \chi_2^0\chi_2^0 \to \chi_1^0\chi_1^0\gamma\gamma$. In principle $e^+e^- \to \chi_2^0\chi_1^0 \to \chi_1^0\chi_1^0\gamma$ could be considered, however the predicted cross section is uninterestingly small. In gravitino LSP models, the CDF event could be explained by $q\bar{q} \to \tilde{e}\tilde{e} \to ee\chi_1^0\chi_1^0 \to ee\tilde{G}\tilde{G}\gamma\gamma$ [8]. In this scenario the best channel for discovery at LEP2 is $e^+e^- \to \chi_1^0\chi_1^0 \to \tilde{G}\tilde{G}\gamma\gamma$. Limits derived from the ALEPH data are compared to the regions favoured by the CDF event within these models. In particular, in the case of GMSB theories, the data are compared to the predictions of the Minimal Gauge-Mediated MGM model of Ref. [8] which assumes that the lightest neutralino is pure bino, that the right-selectron mass is 1.1 times the neutralino mass and that the left-selectron mass is 2.5 times the neutralino mass.

The reaction $e^+e^- \to \gamma\gamma(\gamma)$ proceeds via t-channel electron exchange and has been studied at lower centre-of-mass energies [12]. Deviations from the expected QED differential cross section for the production of two photons could be evidence for new physics due to, for example, $e^+e^-\gamma\gamma$ contact interactions or excited electrons.

This letter is based on an analysis of $58.5\,\mathrm{pb}^{-1}$ of data collected at a luminosity-weighted centre-of-mass energy of 182.7 GeV. Previously published results from ALEPH [1] based on $11.1\,\mathrm{pb}^{-1}$ and $10.6\,\mathrm{pb}^{-1}$ of data taken at 161 GeV and 172 GeV, respectively, are taken into account when setting cross section limits on new physics processes.

2 The ALEPH detector and photon identification

The ALEPH detector and its performance are described in detail elsewhere [13, 14]. The analysis presented here depends largely on the performance of the electromagnetic calorimeter (ECAL). The luminosity calorimeters (LCAL and SICAL), together with the hadron calorimeter (HCAL),

are used mainly to veto events in which photons are accompanied by other energetic particles. The HCAL is instrumented with streamer tubes and, together with the muon chambers, is used to identify muons. The SICAL provides coverage between 34 and 63 mrad from the beam axis while the LCAL provides coverage between 45 and 160 mrad. Each LCAL endcap consists of two halves which fit together around the beam axis; the area where the two halves join is a region of reduced sensitivity ("the LCAL crack"). This vertical crack, which accounts for only 0.05% of the total solid angle coverage of the ALEPH detector, was instrumented with a veto counter for the 183 GeV run. This counter consists of 2 radiation lengths of lead followed by scintillation counters. Energetic electrons (photons) passing through the lead have a greater than 90% (70%) chance of giving a veto signal in the scintillation counters. The tracking system, composed of a silicon vertex detector, wire drift chamber, and time projection chamber (TPC), is used to provide efficient ($> 99.9\%$) tracking of isolated charged particles in the angular range $|\cos\theta| < 0.96$.

The ECAL is a lead/wire-plane sampling calorimeter consisting of 36 modules, twelve in the barrel and twelve in each endcap, which provide coverage in the angular range $|\cos\theta| < 0.98$. Inter-module cracks reduce this solid angle coverage by 2% in the barrel and 6% in the endcaps. However, the ECAL and HCAL cracks are not aligned so there is complete coverage in ALEPH down to 34 mrad. At normal incidence the ECAL comprises a total thickness of 22 radiation lengths and is situated at 185 cm from the interaction point. Anode wire signals, sampled every 512 ns during their rise time, provide a measurement by the ECAL of the interaction time t_0 of the particles relative to the beam crossing with a resolution better than 15 ns for showers with energy greater than 1 GeV. Cathode pads associated with each layer of the wire chambers are connected to form projective "towers", each subtending approximately $0.9^\circ \times 0.9^\circ$. Each tower is read out in three segments in depth "storeys" of four, nine and nine radiation lengths. The high granularity of the calorimeter provides excellent identification of photons and electrons. The energy calibration of the ECAL is obtained from Bhabha and two-photon events. The energy resolution is measured to be $\Delta E/E = 0.18/\sqrt{E} + 0.009$ (E in GeV) [14].

Photon candidates are identified using an algorithm [14] which performs a topological search for localised energy depositions within groups of neighbouring ECAL towers. In order to optimise the energy reconstruction, photons that are not well-contained in the ECAL (near or in a crack) have their energy measured from the sum of the localised energy depositions and all energy deposits in the HCAL within a cone of $\cos\alpha > 0.98$. Photon candidates may also be identified in the tracking system if they convert in the material before the TPC, 6% of a radiation length at normal incidence, producing an electron-positron pair [14].

The trigger most relevant for photonic events is the neutral energy trigger. This trigger is based on the total energy measured on the wires of each of the ECAL modules. For the 183 GeV run, this trigger accepts events if the total wire energy is at least 1 GeV in any barrel module or at least 2.3 GeV in any endcap module. The efficiency of this trigger for the selections presented below is estimated to be at least 99.8%.

3 The Monte Carlo samples

The efficiency for the $e^+e^- \to \nu\bar{\nu}\gamma(\gamma)$ cross section measurement and the background for the anomalous photon plus missing energy searches are estimated using the KORALZ Monte Carlo program [15]. This generator uses the YFS [16] approach to explicitly generate an arbitrary number of initial state photons. It does not however include the small contribution (of order 0.2%) where photons are directly radiated from the W. This Monte Carlo is checked by comparing

to NUNUGG [17] at centre-of-mass energies below the W threshold and to CompHEP [18] at higher energies.

The efficiency estimates for the reaction $e^+e^- \to \gamma\gamma(\gamma)$ are obtained using the GGG generator [19] which contains contributions to order α^3 with both soft and hard photon emission. Events with four hard photons observed in the detector are simulated using an order α^4 generator [20]. The efficiencies for the processes $e^+e^- \to XX$ and $e^+e^- \to XY$ with $X \to Y\gamma$ are estimated using SUSYGEN [21] assuming isotropic production and decay of X and taking into account the effects of initial state radiation.

Background from Bhabha scattering, where initial or final state particles radiate a photon is studied using the UNIBAB [22] Monte Carlo program.

4 One photon and missing energy

4.1 Event selection

The selection of events with one photon and missing energy follows that of the previous ALEPH analysis [1] and only a brief summary is given here. Events are selected with no charged tracks (not coming from a conversion) and exactly one photon inside the acceptance cuts of $|\cos\theta| < 0.95$ with $p_\perp > 0.0375\sqrt{s}$ (where $p_\perp$ is defined as the measured transverse momentum relative to the beam axis). Cosmic ray events that traverse the detector are eliminated by the charged track requirement or if there are hits in the outer part of the HCAL. Residual cosmic ray events and events with detector noise in the ECAL are removed by selection criteria based on the ECAL information. The "impact parameter of the photon", calculated using the barycentre of the photon shower in each of the three ECAL storeys, is required to be less than 25 cm. The compactness of the shower in the ECAL is calculated by taking an energy-weighted average of the angle subtended at the interaction point between the cluster barycentre and the barycentre of each of the ECAL storeys contributing to the cluster. The compactness is required to be less than 0.85°. The interaction time of the event is required to be consistent with a beam crossing.

To suppress background from Bhabha scattering, events are required to have no energy deposited within 14° of the beam axis and to have less than 1 GeV of non-photonic energy. The selection is modified to take advantage of the LCAL veto counters installed prior to the 183 GeV run. The requirement that events with missing momentum around the LCAL crack region have a $p_\perp > 0.145\sqrt{s}$ is replaced by the requirement that there is no veto signal detected in the LCAL veto counters.

4.2 Measurement of the $e^+e^- \to \nu\bar{\nu}\gamma(\gamma)$ cross section

The efficiency of the above selection for the process $e^+e^- \to \nu\bar{\nu}\gamma(\gamma)$ is estimated from the Monte Carlo to be 77%. This efficiency includes a 2% loss, due to uncorrelated noise or beam-related background in the detector, estimated using events triggered at random beam crossings.

When this selection is applied to the data, 195 one-photon events are found. The KORALZ Monte Carlo predicts that 187 events would be expected from Standard Model processes. The cross section to have at least one photon inside the acceptance $|\cos\theta| < 0.95$ and $p_\perp > 0.0375\sqrt{s}$ is measured to be

$$\sigma(e^+e^- \to \nu\bar{\nu}\gamma(\gamma)) = 4.32 \pm 0.31 \pm 0.13\,\text{pb}.$$

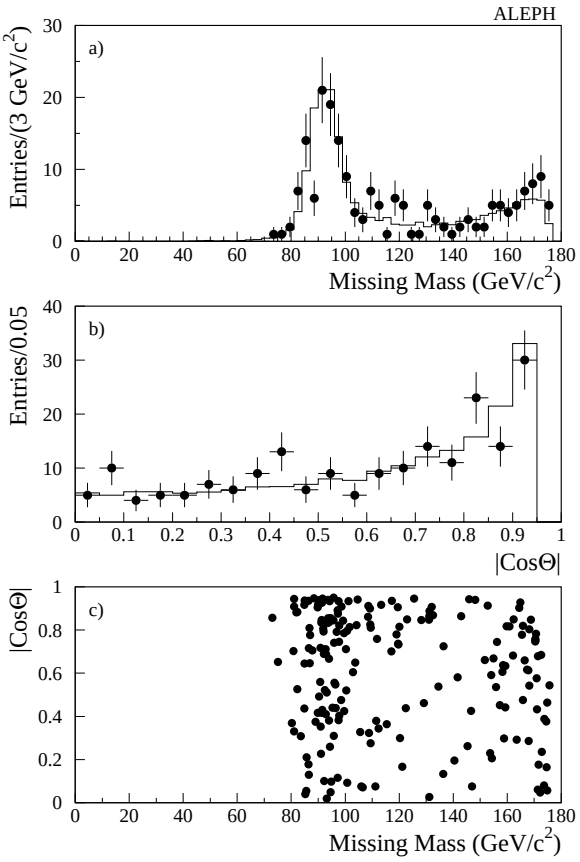

Figure 1: *a) The invariant mass distribution of the system recoiling against the photon candidate is shown for the data (points with error bars) and Monte Carlo (histogram). b) The* $|\cos\theta|$ *distribution is shown for the data (points with error bars) and Monte Carlo (histogram). c) The invariant mass of the system recoiling against the photon candidate versus* $|\cos\theta|$ *is shown for the data.*

The missing mass and polar angle distributions of the selected data events are in good agreement with the Monte Carlo expectations as shown in Figure 1 [1].

The estimate of the systematic uncertainty in the above cross section includes contributions from the sources listed in Table 1. The simulation of the energetic photon shower is checked with a sample of Bhabha events selected requiring two collinear beam-momentum tracks and using muon chamber information to veto $\mu^+\mu^-$ events. The tracking information is masked from these events and the photon reconstruction is redone. The efficiency to reconstruct a photon in the data is found to be consistent at the 0.6% level with that predicted by the simulation. The uncertainty in the number of simulated pair conversions is estimated to give a 0.3% change in the overall efficiency. The 1% energy calibration uncertainty is found to have a negligible effect. The level of cosmic ray and detector noise background is measured by looking for events slightly out-of-time with respect to the beam crossing. No out-of-time events are observed in a time window five times larger than that used in the selection. This leads to an estimate of less than 0.2 events

[1] Colour versions of the figures in this paper are available in encapsulated postscript form at **http://alephwww.cern.ch/ALPUB/paper/paper.html**

Table 1: *Systematic uncertainties for the one-photon channel.*

Source	Uncertainty (%)
Photon selection	0.6
Converted photon selection	0.3
Background	<0.2
Integrated luminosity	0.5
Monte Carlo theoretical	3.0
Monte Carlo statistical	0.4
Total (in quadrature)	3.1

expected in the selected sample. The residual background from Bhabha scattering is estimated from Monte Carlo studies and is found to be negligible. From a comparison of different event generators the theoretical uncertainty on the selection efficiency is estimated to be less than 3%. The total systematic uncertainty is obtained by adding in quadrature the individual contributions.

4.3 Search for the process $e^+e^- \to XY \to YY\gamma$

In order to search for the signal $e^+e^- \to XY \to YY\gamma$, a two-dimensional binned maximum likelihood fit is performed on the observed missing mass versus $\cos\theta$ spectrum under the hypothesis that there is a mixture of signal and background in the data. Details of the fitting procedure are given in Ref. [1]. Data recorded at 161 GeV and 172 GeV [1] are included in the fit with a β/s cross section dependence. The fit is performed for all possible X,Y mass combinations in steps of $1\,\mathrm{GeV}/c^2$ and the resulting upper limits on the cross section at 95% C.L. are shown in Figure 2.

4.4 Search for the process $e^+e^- \to \tilde{G}\tilde{G}\gamma$

If the gravitino $\tilde{G}$ is very light the cross section for the process $e^+e^- \to \tilde{G}\tilde{G}\gamma$ can become appreciable. In order to search for this process a binned maximum likelihood fit is performed as above. In this case the missing mass and $\cos\theta$ distributions of the signal together with the cross section dependence on the centre-of-mass energy are calculated from the differential cross section given in Ref. [9]. From the fit a cross section limit of 0.38 pb at $\sqrt{s} = 183$ GeV is obtained at 95% C.L. This results in a 95% C.L. lower limit of $8.3 \times 10^{-6}\,\mathrm{eV}/c^2$ for the mass of the gravitino [9]. In the same paper a more general approach gives a mass limit dependent on two free parameters. In the worst case this would lead to a limit on the gravitino mass lower by factor two. The systematic uncertainty of 3.1% is taken into account by means of the method of Ref. [23] and is found to have a negligible effect on the above mass limit.

5 Two photons and missing energy

5.1 Event preselection

As described in the introduction, there are two SUSY scenarios which can give acoplanar photons: the gravitino LSP and neutralino LSP scenarios. The signals differ in that the invisible particle is essentially massless in the first scenario and can have substantial mass in the second one. This

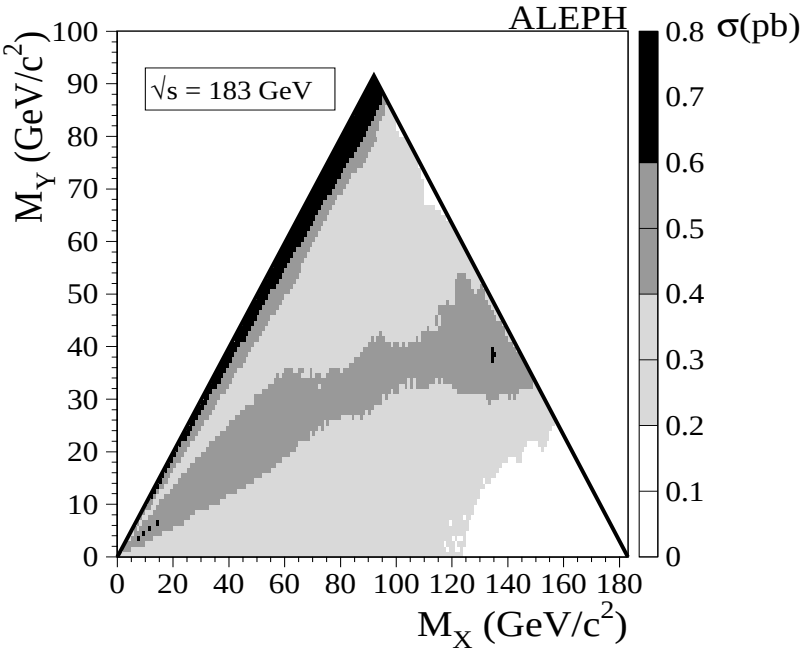

Figure 2: *The 95% C.L. upper limit on the production cross section in pb for the process* $e^+e^- \to XY \to YY\gamma$. *The limits are valid for* $\sqrt{s} = 183\,\mathrm{GeV}$ *assuming a* β/s *threshold dependence, isotropic decays, short X lifetime* ($\tau_X < 0.1\,\mathrm{ns}$) *and* 100% *branching ratio for* $X \to Y\gamma$.

leads to two slightly different search criteria, as described in the subsections below. However the similarity between the two scenarios allows a common preselection of events with two photons and missing energy. Events are selected with no charged tracks (not coming from a conversion) and at least two photons, with energy above 1 GeV, inside the acceptance of $|\cos\theta| < 0.95$. Since at least two photons are required, background from cosmic rays and detector noise is less severe, so the impact parameter and compactness requirements are not imposed. Events with more than two photons are required to have at least $0.4\sqrt{s}$ of missing energy. Background from the process $e^+e^- \to \gamma\gamma(\gamma)$ is effectively eliminated by requiring that the acoplanarity of the two most energetic photons be less than 177° and that there be less than 1 GeV of additional visible energy in the event. The total $p_\perp$ is required to be greater than 3.75% of the missing energy, reducing background from radiative events with final state particles escaping down the beam axis to a negligible level.

When this preselection is applied to the 183 GeV data, 9 events are selected while 10.8 are predicted from the process $e^+e^- \to \nu\bar{\nu}\gamma(\gamma)$. This prediction is only known with an accuracy of around ±10%. The missing mass and the energy of the second most energetic photon of these selected data events, and 3 events selected at lower centre-of-mass energies [1], are shown together with Monte Carlo expectations in Figure 3.

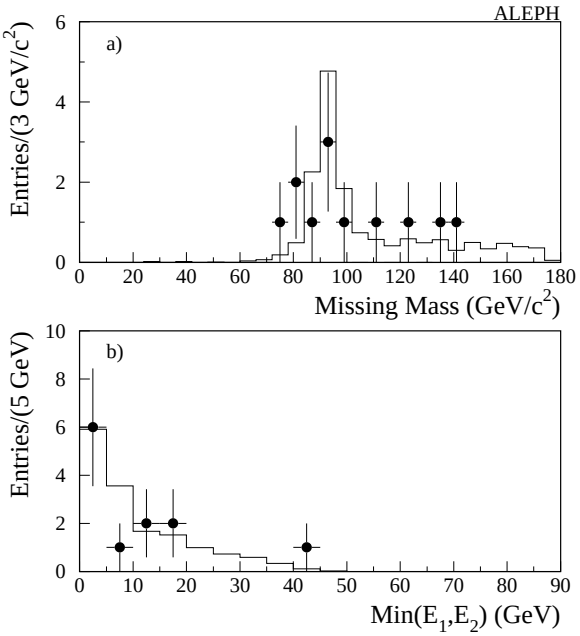

Figure 3: *a) The invariant mass distribution of the system recoiling against the photon candidates is shown for the data (points with error bars) and Monte Carlo (histogram). b) The distribution of the energy of the second most energetic photon is shown for the data (points with error bars) and Monte Carlo (histogram). Both plots contain data taken from centre-of-mass energies in the range* 161 GeV *to* 183 GeV.

5.2 Search for the process $e^+e^- \to XX \to YY\gamma\gamma$: Y massless

For this topology one additional cut is placed on the energy of the less energetic photon E_2 to substantially reduce the remaining Standard Model background. The energy distribution of the second most energetic photon is peaked near zero for the background, whereas for the signal both photons have a flat distribution in an interval depending on the neutralino mass and the centre-of-mass energy. This cut is placed at $E_2 > 25$ GeV (this is the optimised value in the MGM [8] model). After this final cut is applied one event is found in the 183 GeV data while 1.43 events are expected from background processes. Applying this increased E_2 cut to the previously analysed data taken at 161 GeV to 172 GeV no events are observed in the data while 0.35 are expected from background processes. The upper limit on the production cross section at 183 GeV, obtained without performing background subtraction, is in the range of 0.10–0.12 pb for a 100% $X \to Y\gamma$ branching ratio and X masses in the range 45 GeV/c^2 to 90 GeV/c^2. The data recorded at lower energies are also used in the evaluation of this limit. The integrated luminosities are scaled according to the cross section predictions of the MGM [8] model. The mass limit obtained for this model is

$$M_{\chi_1^0} \geq 84\,\mathrm{GeV/c^2}$$

at 95% C.L. for a neutralino with lifetime < 3 ns. The systematic uncertainty for this analysis is estimated to be 2%, dominated by the photon reconstruction efficiency. The effect of this

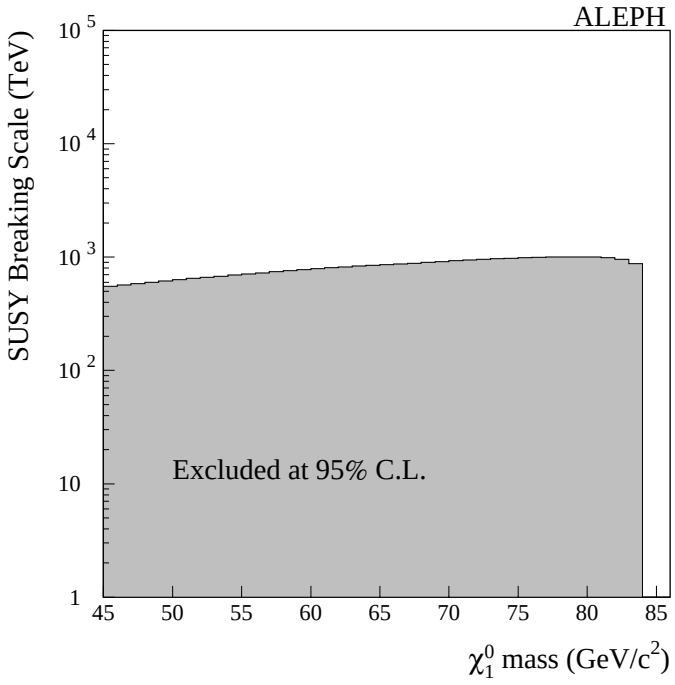

Figure 4: *The excluded region of the MGM model [8] in the neutralino mass, $\sqrt{F}$ plane.*

uncertainty on the cross section upper limit is less then 1% when taken into account by means of the method of Ref. [23]. The effect on the mass limit is negligible.

In the GMSB model the neutralino can have a non-negligible lifetime which depends directly on the SUSY breaking scale $\sqrt{F}$. The lifetime of the neutralino is given by [7]

$$c\tau \simeq 130 \left(\frac{100\,\mathrm{GeV/c^2}}{\mathrm{M}_{\chi_1^0}} \right)^5 \left(\frac{\sqrt{\mathrm{F}}}{100\ \mathrm{TeV}} \right)^4 \mu\mathrm{m}.$$

The efficiency due to lifetime ϵ_τ to reconstruct a photon resulting from a neutralino decay of a given lifetime is found to be well parameterised by $\epsilon_\tau = 1 - \exp(-l/\gamma\beta c\tau)$, where the average distance l for reconstruction is 2.5 m. The 95% C.L. exclusion limit obtained in the $\sqrt{F}$, $\mathrm{M}_{\chi_1^0}$ plane using this parameterisation is shown in Figure 4. For a neutralino of mass 84 GeV/c^2 and lifetime 3 ns, the SUSY breaking scale is at least 730 TeV at 95% C.L.

At LEP2 the production of bino neutralinos would proceed via t-channel selectron exchange. Right-selectron exchange dominates over left-selectron exchange. Thus, the cross section for $\mathrm{e^+e^-} \to \chi_1^0\chi_1^0$ depends strongly on the right-selectron mass. The theoretical cross section for $\mathrm{e^+e^-} \to \chi_1^0\chi_1^0$ is calculated at each $\mathrm{M}_{\tilde{e}_R}$, $\mathrm{M}_{\chi_1^0}$ mass point for right-selectron masses ranging from 70 GeV/c^2 to 200 GeV/c^2 and neutralino masses ranging from 30 GeV/c^2 to 86 GeV/c^2 and compared to the experimental limit to obtain the exclusion region. The neutralino mass limits are also evaluated for various left-selectron masses. The result is found to be robust at the $\pm$1 GeV/c^2 level for left-selectron masses ranging from $\mathrm{M}_{\tilde{e}_L} = \mathrm{M}_{\tilde{e}_R}$ to $\mathrm{M}_{\tilde{e}_L} \gg \mathrm{M}_{\tilde{e}_R}$.

The experimentally excluded region in the neutralino, selectron mass plane is shown in Figure 5.

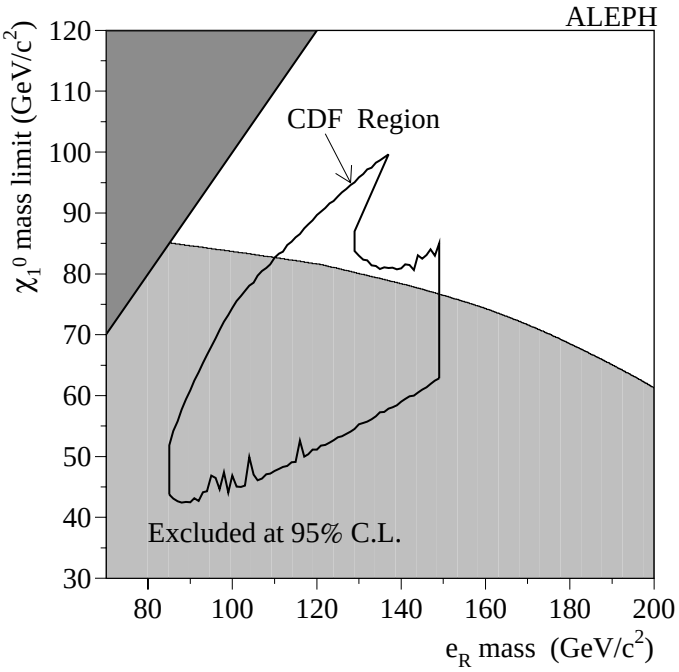

Figure 5: *The excluded region in the neutralino, selectron mass plane at 95% C.L. for a pure bino neutralino (light shaded area). Overlayed is the CDF region determined from the properties of the CDF event assuming the reaction* $\mathrm{q\bar{q}} \to \tilde{\mathrm{e}_\mathrm{R}}\tilde{\mathrm{e}_\mathrm{R}} \to \mathrm{ee}\chi_1^0\chi_1^0 \to \mathrm{ee}\tilde{\mathrm{G}}\tilde{\mathrm{G}}\gamma\gamma$ *(taken from the Ref. [25]). The dark shaded region corresponds to a topology not covered by this analysis.*

Overlayed is the "CDF region", the area in the neutralino, selectron mass plane where the properties of the CDF event are compatible with the process $\mathrm{q\bar{q}} \to \tilde{\mathrm{e}_\mathrm{R}}\tilde{\mathrm{e}_\mathrm{R}} \to \mathrm{ee}\chi_1^0\chi_1^0 \to \mathrm{ee}\tilde{\mathrm{G}}\tilde{\mathrm{G}}\gamma\gamma$ (taken from Ref. [25]). Most of the CDF region is excluded at 95% C.L. by this analysis.

5.3 Search for the process $\mathrm{e^+e^-} \to \mathrm{XX} \to \mathrm{YY}\gamma\gamma$: Y massive

For massive Y a simple energy cut is not optimal since the photons from the $\mathrm{X} \to \mathrm{Y}\gamma$ decay can have low energy. Here the fact that the $\mathrm{e^+e^-} \to \nu\bar{\nu}\gamma(\gamma)$ background peaks at small polar angles and has a missing mass near the Z mass is utilised. Events that have missing mass between $82\,\mathrm{GeV}/c^2$ and $100\,\mathrm{GeV}/c^2$ and the energy of the second most energetic photon less than 10 GeV are rejected. The $\cos\theta$ cut is set using the $\bar{\mathrm{N}}_{95}$ procedure, leading to a requirement of $|\cos\theta| < 0.8$. When this selection is applied to the 183 GeV data 3 events are selected while 2.8 events are expected from the $\mathrm{e^+e^-} \to \nu\bar{\nu}\gamma(\gamma)$ process. The upper limits obtained on the cross section as a function of the masses of X and Y are shown in Figure 6. These upper limits are derived without performing background subtraction but the observed candidates are taken into account only where they are kinematically consistent with a given X,Y mass pairing. They are derived taking into account lower energy data [1] with a β/s threshold dependence and assuming a branching ratio for $\mathrm{X} \to \mathrm{Y}\gamma$ of 100%. The systematic uncertainties for this analysis are the same as for the massless Y scenario and the effect on the upper limits is again less than 1%.

The χ_1^0 LSP interpretation of the CDF event (along with the non-observation of other SUSY

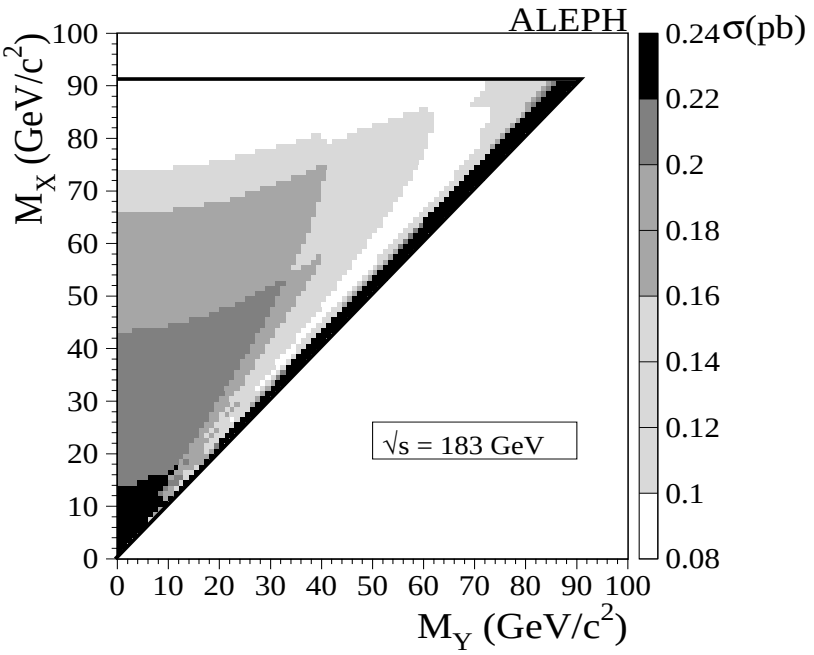

Figure 6: *The 95% C.L. upper limit on the production cross section in pb for the process* $e^+e^- \to XX \to YY\gamma\gamma$ *multiplied by* $\mathcal{B}(X \to Y\gamma)$ *squared. The limit is valid for* $\sqrt{s} = 183\,\mathrm{GeV}$ *assuming* β/s *threshold behaviour and isotropic decays.*

signatures at Fermilab) suggests a high branching ratio for $\chi_2^0 \to \chi_1^0\gamma$. A 100% branching ratio is achieved when the χ_2^0 is pure photino and the χ_1^0 is pure higgsino. In this scenario, the lower mass limit of χ_2^0 as a function of the selectron mass is calculated and compared to the region compatible with the CDF event. In Figure 7 two scenarios $M_{\tilde{e}_L} = M_{\tilde{e}_R}$ and $M_{\tilde{e}_L} \gg M_{\tilde{e}_R}$ are shown. With the assumption that the χ_2^0 is pure photino and the χ_1^0 is pure higgsino, these results exclude a significant portion of the region compatible with the kinematics of the CDF event given by the neutralino LSP interpretation.

6 Hard collinear photons

6.1 Event selection and the process $e^+e^- \to \gamma\gamma(\gamma)$

An acceptance for events from the process $e^+e^- \to \gamma\gamma(\gamma)$ is defined to include events with at least two photons with polar angles such that $|\cos\theta| < 0.95$ and energies above $0.25\sqrt{s}$ where the angle between the two most energetic photons is at least 160°. The background from Bhabha scattering is greatly reduced by allowing at most one converted photon per event and requiring that there be no tracks in the event not associated with that photon. Cosmic ray events which traverse the detector are eliminated if they leave hits in the outer part of the HCAL or if their measured interaction time is inconsistent with a beam crossing. The efficiency of this selection for events within the acceptance is 84%.

The above selection is applied to the three data samples collected at centre-of-mass energies

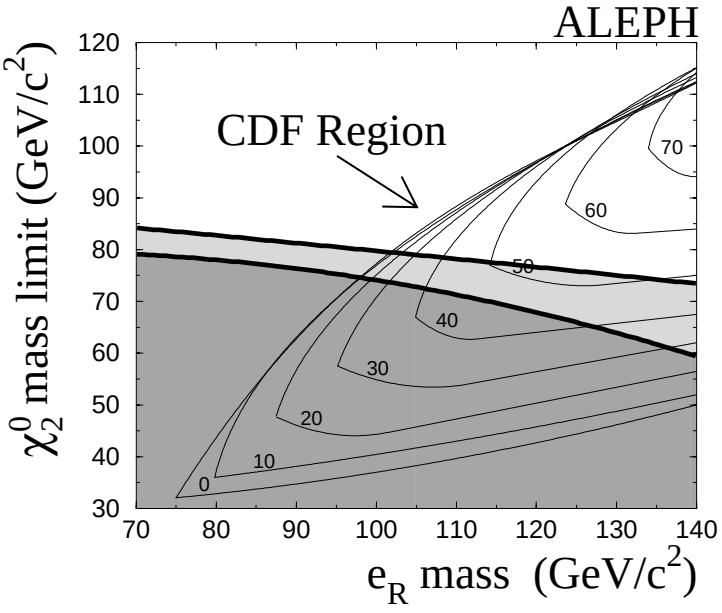

Figure 7: *The excluded region in the neutralino, selectron mass plane at 95% C.L. For this plot it is assumed that the χ_2^0 is pure photino and that the χ_1^0 is pure higgsino which implies $\mathcal{B}(\chi_2^0 \to \chi_1^0\gamma) = 1$. The lightly shaded region is for $M_{\tilde{e}_L} = M_{\tilde{e}_R}$. The darker shaded region refers to $M_{\tilde{e}_L} \gg M_{\tilde{e}_R}$. The mass limit is independent of the χ_1^0 mass as long as the $\chi_2^0 - \chi_1^0$ mass differences is greater than $25\,\mathrm{GeV}/c^2$. Overlayed is the CDF region labelled by the mass of χ_1^0 in GeV/c^2. This is the area determined from the properties of the CDF event assuming the reaction $q\bar{q} \to \tilde{e}\tilde{e} \to ee\chi_2^0\chi_2^0 \to ee\chi_1^0\chi_1^0\gamma\gamma$ (taken from Ref. [5]).*

Table 2: *The selected number of observed and expected events which have two or more (three or more) photons inside the acceptance, the number of expected background events and the measured and theoretical cross sections at the three different centre-of-mass energies.*

$\sqrt{s}$	Observed	Expected	Exp. Bkg.	Cross Section (pb)	Theor. Cross Section (pb)
161	114 (7)	124 (6.4)	1	$12.0 \pm 1.1 \pm 0.2$	$13.20 \pm 0.14 \pm 0.13$
172	99 (1)	103 (5.3)	1	$11.0 \pm 1.1 \pm 0.2$	$11.59 \pm 0.13 \pm 0.12$
183	500 (25)	496 (26.3)	4	$10.1 \pm 0.5 \pm 0.2$	$10.11 \pm 0.11 \pm 0.10$

of 161 GeV, 172 GeV and 183 GeV. The number of events observed and expected at each of the energies is given in Table 2. Summed over the three centre-of-mass energies a total of 713 events are selected in good agreement with the total Monte Carlo prediction of 729 events, six of which are expected to come from the residual Bhabha background [22]. Also given in Table 2 are the number of observed and expected events that have one or more additional photons with energy above 1 GeV inside the angular range $|\cos\theta| < 0.95$. A total of 33 such events are observed, consistent with the expectation of 38 events. Two events are observed in the data with four photons in agreement with a Monte Carlo [20] expectation of 1.4 events. No events are observed with more than four photons.

The lowest order differential cross section for electron-positron annihilation into two photons

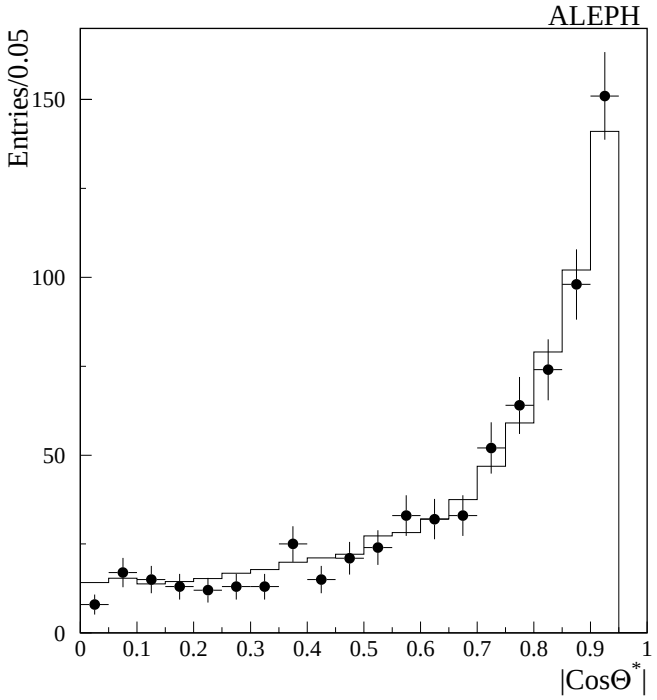

Figure 8: *Predicted and observed lowest-order differential cross section as a function of* $\cos\theta^*$ *for the reaction* $e^+e^- \to \gamma\gamma$. *The predicted distribution includes a small contribution from the Bhabha background. The errors shown here are purely statistical.*

is given by

$$\left(\frac{d\sigma}{d\Omega}\right)_{\rm Born} = \frac{\alpha^2}{s}\left(\frac{1+\cos^2\theta}{1-\cos^2\theta}\right).$$

The observed cross section is modified by two effects: higher order processes, in particular initial state radiation, and detector effects. Due to initial state radiation, the centre-of-mass frame of the two detected photons is not necessarily at rest in the laboratory. The events are therefore transformed into the two-photon rest frame to define the production angle θ^* appropriately. The distribution of this production angle is in good agreement between data and Monte Carlo expectations ($\chi^2 = 17$ for 19 degrees of freedom) as shown in Figure 8. The background-subtracted cross section for events inside the acceptance is given in Table 2.

The systematic uncertainty in the above cross section estimates includes contributions from the various sources listed in Table 3. The uncertainties coming from the photon selection efficiency are measured as in the single photon analysis. The uncertainty in the level of the Bhabha background is conservatively estimated to be equal to 100% of the measured background of 0.8%. The effect of missing higher orders in the Monte Carlo is estimated to be less than 1.0%. This estimate is obtained by comparing the number of observed and selected events in a high statistics data sample recorded at the Z peak. Added in quadrature, the total systematic uncertainty is 2.2%. It is treated as an uncertainty in the overall normalisation of the data.

Table 3: *Systematic uncertainties in the* $e^+e^- \to \gamma\gamma$ *analysis.*

Source	Uncertainty (%)
Photon selection	1.2
Converted photon selection	0.6
Background	0.8
Integrated luminosity	0.5
Monte Carlo statistical	1.1
Monte Carlo theoretical	< 1.0
Total (in quadrature)	2.2

6.2 QED cutoff parameters

Possible deviations from QED are usually characterised by cutoff parameters Λ_+ and Λ_- corresponding to a modified differential cross section

$$\frac{\mathrm{d}\sigma}{\mathrm{d}\Omega} = \left(\frac{\mathrm{d}\sigma}{\mathrm{d}\Omega}\right)_{\mathrm{QED}} \left[1 \pm \frac{s^2}{2\Lambda_\pm^4}(1-\cos^2\theta^*)\right].$$

In order to extract limits on the parameters Λ_+ and Λ_- a binned maximum likelihood fit is performed on the background-subtracted $\cos\theta^*$ distribution under the assumption that it contains contributions from both QED and the cutoff interaction. Since the $\cos\theta^*$ distribution of the cutoff interaction is only known to lowest order, a bin-by-bin correction is made by comparing the third order QED distribution to the corresponding lowest order distribution. This assumes that the effect of higher order corrections is the same for both QED and the new physics. A further bin-by-bin correction is made to take into account the detector efficiency. The limit on Λ_+ (Λ_-) is obtained by integrating the likelihood distribution over the physically allowed region $\Lambda_+ > 0$ ($\Lambda_- > 0$). The 95% C.L. lower limits obtained for Λ_+ and Λ_- are 270 GeV and 230 GeV, respectively. The systematic uncertainties are taken into account using the method of Ref. [23] and are found to have a negligible effect on the limits. Figure 9 shows the ratio of the observed cross section to that predicted by QED, as a function of $\cos\theta^*$. Also indicated, as dotted lines, are the modified cross sections corresponding to the 95% C.L. lower limits on Λ_+ and Λ_-.

6.3 Contact interactions

An alternative description of extensions to QED is provided by effective Lagrangians, which contain non-standard couplings of the form γe^+e^- and $\gamma\gamma e^+e^-$. The lowest order effective Lagrangians, describing these interactions, contain operators of order 6, 7 and 8. These lead to modified differential cross sections of the form [26]

$$\begin{aligned}
\left(\frac{\mathrm{d}\sigma}{\mathrm{d}\Omega}\right)_{\mathrm{QED+6}} &= \left(\frac{\mathrm{d}\sigma}{\mathrm{d}\Omega}\right)_{\mathrm{QED}} \left[1 + \frac{s^2}{\alpha\Lambda_6^4}(1-\cos^2\theta^*)\right], \\
\left(\frac{\mathrm{d}\sigma}{\mathrm{d}\Omega}\right)_{\mathrm{QED+7}} &= \left(\frac{\mathrm{d}\sigma}{\mathrm{d}\Omega}\right)_{\mathrm{QED}} + \frac{s^2}{32\pi\Lambda_7^6}, \\
\left(\frac{\mathrm{d}\sigma}{\mathrm{d}\Omega}\right)_{\mathrm{QED+8}} &= \left(\frac{\mathrm{d}\sigma}{\mathrm{d}\Omega}\right)_{\mathrm{QED}} + \frac{s^2 m_{\mathrm{e}}^2}{32\pi\Lambda_8^8}.
\end{aligned}$$

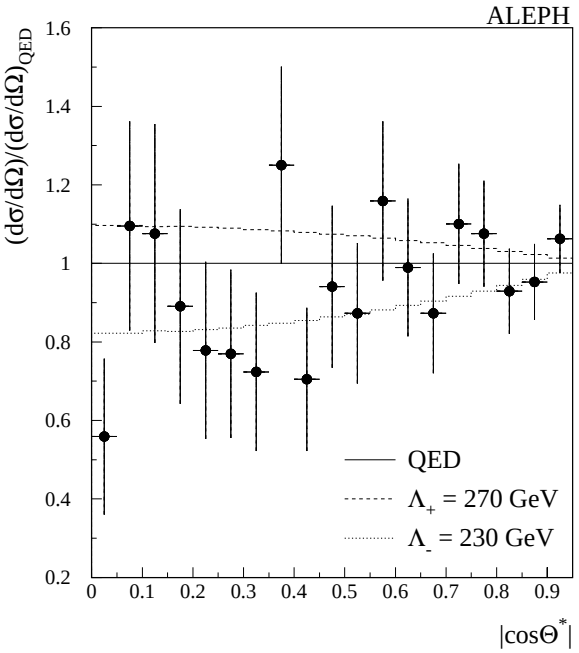

Figure 9: *The ratio of the observed to predicted cross sections, for the process* $e^+e^- \to \gamma\gamma(\gamma)$*, as a function of* $\cos\theta^*$*. Also shown are the 95% C.L. level limits on the QED cutoff model.*

Fits are performed to extract limits on these parameters using the procedure outlined above. The 95% C.L. lower limits obtained for Λ_6, Λ_7 and Λ_8 are 1100 GeV, 624 GeV and 18.8 GeV, respectively. The systematic uncertainties are again found to have a negligible effect on the limits.

6.4 Limits on M_{e^*}

The reaction $e^+e^- \to \gamma\gamma$ can also proceed via the exchange of an excited electron. In this case the cross section depends on two parameters: the mass M_{e^*} of the excited electron and the $ee^*\gamma$ coupling. The simplest gauge-invariant form [27] of the interaction (the Low Lagrangian) leads to the differential cross section given in [28]. A fit is performed as above and a 95% C.L. lower limit on M_{e^*} of 250 GeV/c^2 is obtained in the case of equal $ee^*\gamma$ and $ee\gamma$ couplings.

7 Conclusions

Single- and multi-photon production is studied in the ALEPH data collected at centre-of-mass energies up to 183 GeV. The cross sections for the processes $e^+e^- \to \nu\bar{\nu}\gamma(\gamma)$ and $e^+e^- \to \gamma\gamma(\gamma)$ are measured and are found to be compatible with the expectations of the Standard Model.

The data from the photon(s) and missing energy analyses are used to derive cross section upper limits for the processes $e^+e^- \to XY \to YY\gamma$, $e^+e^- \to \tilde{G}\tilde{G}\gamma$ and $e^+e^- \to XX \to YY\gamma\gamma$. A cross section upper limit of 0.38 pb is obtained of the $e^+e^- \to \tilde{G}\tilde{G}\gamma$ process. From this cross section upper limits a 95% C.L. lower limit of 8.3×10^{-6} eV/c^2 at 95% C.L. is set on the mass of the gravitino [9]. In the context of the MGM model [8] a 95% C.L. lower limit on the χ_1^0 mass is

found to be $84\,\mathrm{GeV}/c^2$ ($\tau_{\chi_1^0} < 3\,\mathrm{ns}$). The lower limit on the χ_1^0 (χ_2^0) mass as a function of selectron mass is determined and compared to the region compatible with the CDF event for the gravitino (neutralino) LSP scenario.

The data from the hard collinear photon analysis are used to place limits on the parameters of a number of extensions to the Standard model, notably the presence of $\mathrm{e^+e^-}\gamma\gamma$ contact interactions and the exchange of a massive excited electron in the t-channel. The 95% C.L. lower limits on the QED cutoff parameters Λ_+ and Λ_- are found to be 270 GeV and 230 GeV, respectively. The effect of excited electron exchange depends on both the mass and coupling constant. In the simplest case, an assumption that the $\mathrm{ee^*}\gamma$ coupling is equal to the $\mathrm{ee}\gamma$ coupling yields a 95% C.L. lower limit on $M_{\mathrm{e^*}}$ of $250\,\mathrm{GeV}/c^2$.

Acknowledgements

We wish to congratulate our colleagues in the CERN accelerator divisions for their very successful operation of the LEP storage ring. We are grateful to the engineers and technicians in all our institutions for their contribution towards the excellent performance of ALEPH. Those of us from non-member countries thank CERN for its hospitality.

References

[1] ALEPH Collaboration, CERN-PPE/97-122, submitted to Phys. Lett. **B**.

[2] JADE Collaboration, Phys. Lett. **B139** (1984) 327;
MAC Collaboration, Phys. Rev. **D33** (1986) 3472;
CELLO Collaboration, Phys. Lett **B215** (1988) 186;
VENUS Collaboration, Z. Phys **C45** (1989) 175;
ASP Collaboration, Phys. Rev. **D39** (1989) 3207;
TOPAZ Collaboration, Phys. Lett. **B361** (1995) 199;
DELPHI Collaboration, Eur. Phys. J. **C1** (1998) 1;
L3 Collaboration, CERN-PPE/97-76, submitted to Phys. Lett. **B**;
OPAL Collaboration, CERN-PPE/97-132, submitted to Z. Phys. C.

[3] H. Komatsu and J. Kumo, Phys. Lett. **B157** (1985) 90.

[4] H. Haber and D. Wyler, Nucl. Phys. **B323** (1989) 267.

[5] S. Ambrosanio et al., Phys. Rev. **D55** (1997) 1372.

[6] P. Fayet, Phys. Lett. **B69** (1977) 489, **B70** (1977) 461;
M. Dine, W. Fischler and M. Srednichi, Nucl. Phys. **B189** (1981) 575;
M. Dine, A. Nelson and Y. Shirman, Phys. Rev. **D51** (1995) 1362;
S. Dimopoulos, S. Thomas and J. D. Wells, Nucl. Phys. **B488** (1997) 39.

[7] S. Dimopoulos et al., Phys. Rev. Lett. **76** (1996) 3494.

[8] S. Dimopoulos, S. Thomas and J. D. Wells, Phys. Rev. **D54** (1996) 3283.

[9] A. Brignole, F. Feruglio and F. Zwirner, CERN-TH/97-339.

[10] CDF Collaboration, HEP-EX/9801019, submitted to Phys. Rev. Lett.

[11] D0 Collaboration, Phys. Rev. Lett. **80** (1998) 442.

[12] PLUTO Collaboration, Phys. Lett. **B59** (1980) 87;
JADE Collaboration, Z. Phys. **C19** (1983) 197;
MARKJ Collaboration, Phys. Rev. Lett. **53** (1984) 134;
TASSO Collaboration, Z. Phys. **C26** (1984) 337;
CELLO Collaboration, Phys. Lett. **B168** (1986) 420;
HRS Collaboration, Phys. Rev. **D34** (1986) 3286;
MAC Collaboration, Phys. Rev. **D35** (1987) 1;
VENUS Collaboration, Z. Phys. **C45** (1989) 175;
TOPAZ Collaboration, Phys. Lett. **B284** (1992) 144;
AMY Collaboration, Phys. Lett. **B303** (1993) 385;
DELPHI Collaboration, Phys. Lett. **B327** (1994) 386;
ALEPH Collaboration, Phys. Lett. **B384** (1996) 333;
L3 Collaboration, Phys. Lett. **B413** (1997) 159;
OPAL Collaboration, Eur. Phys. J. **C1** (1998) 21.

[13] ALEPH Collaboration, Nucl. Instrum. Methods **A294** (1990) 121.

[14] ALEPH Collaboration, Nucl. Instrum. Methods **A360** (1995) 481.

[15] S. Jadach, B. F. L. Ward and Z. Was, Comp. Phys. Commun. **79** (1994) 503.

[16] D. R. Yennie, S. C. Frautschi and H. Suura, Annals of Phys. **13** (1961) 379.

[17] R. Miquel, C.Mana and M. Martinez, Z. Phys. **C48** (1990) 309.

[18] E. Boos et al., preprint INP MSU-94-36/358 (1995), hep-ph/9503280

[19] F. A. Berends and R. Kleiss, Nucl. Phys. **B186** (1981) 22.

[20] P. Janot, Tests of QED to O(α^3) and O(α^4) and a search for excited leptons, using the CELLO detector at PETRA, Ph.D. Thesis, LAL 87-31 (1987).

[21] S. Katsanevas and S. Melachroinos, in *Physics at LEP2*, Eds. G. Altarelli, T. Sjöstrand, F. Zwirner, CERN Report 96-01, Volume 2 (1996) 328.

[22] H. Anlauf et al., Comp. Phys. Commun. **79** (1994) 466.

[23] R. D. Cousins and V. L. Highland, Nucl. Instrum. Methods **A320** (1992) 331.

[24] G. F. Grivaz and F. Le Diberder, LAL 92-37 (1992).

[25] J. Lopez and D. Nanopoulos, Phys. Rev. **D55** (1997) 4450.

[26] O. J. P. Eboli et al., Phys. Lett. **B271** (1991) 274.

[27] F. E. Low, Phys. Rev. Lett. **14** (1965) 238.

[28] A. Litke, Experiments with electron-positron colliding beams, Ph.D. Thesis, Harvard Univ (1970).